Scilight

SustEnergMat

https://www.sciltp.com/journals/sem

Article

CuproGraf: Towards Readily Accessible Copper of Enhanced Electrical Conductivity

Matteo Formenti [1], Rosaria Ciriminna [2,*], Giorgia Lupi [3], Carlo Fanciulli [4], Cristina Della Pina [1,5,*], Riccardo Casati [3,*] and Mario Pagliaro [2,*]

[1] Dipartimento di Chimica, Università degli Studi di Milano, via Golgi 19, 20133 Milano, Italy
[2] Istituto per lo Studio dei Materiali Nananostrutturati, CNR, via U. La Malfa 153, 90146 Palermo, Italy
[3] Dipartimento di Ingegneria Meccanica, Politecnico di Milano, via G. La Masa 1, Ed. B22, 20156 Milano, Italy
[4] Istituto di Chimica della Materia Condensata e di Tecnologie per l'Energia, CNR, via G. Previati 1/e, 23900 Lecco, Italy
[5] Consorzio Interuniversitario Nazionale per la Scienza e Tecnologia dei Materiali, via Giusti 9, 50121, Firenze, Italy
* Correspondence: rosaria.ciriminna@cnr.it (R.C.); cristina.dellapina@unimi.it (C.D.P.); riccardo.casati@polimi.it (R.C.); mario.pagliaro@cnr.it (M.P.)

How To Cite: Formenti, M.; Ciriminna, R.; Lupi, G.; et al. CuproGraf: Towards Readily Accessible Copper of Enhanced Electrical Conductivity. *SustEnergMat* **2026**, *1*(1), 1.

Received: 3 October 2025
Revised: 1 December 2025
Accepted: 2 December 2025
Published: 9 December 2025

Abstract: Graphene was encapsulated within the crystal lattice of Cu via the chemical route to molecularly doped metals affording an excellent electrical conductor dubbed herein "CuproGraf". Metal bars in CuproGraf embedding less than 0.5 wt% graphene obtained by heating followed by hot rolling show nearly 7% lower resistivity when compared to a copper bar obtained from pure Cu powder using the same non-optimized hot rolling procedure. Considering the ease of CuproGraf preparation, and that substantial room for improvement exists by adopting a different CuproGraf powder sintering route to produce bulk wires and foils, the method is promising towards replacement of silver-plated copper wires or similar enhanced conductors wherein higher conductivity than that of copper is required.

Keywords: conductivity; CuproGraf; molecularly doped metal; copper; graphene

1. Introduction

Copper is widely used to produce all sort of electrical wires and electrical circuits due to its good electrical conductivity, abundance, low cost and excellent physical and mechanical properties including malleability and durability which allow it to be easily formed into wires while efficiently conducting electricity [1]. Research on advanced electrical conductors that outperform copper and aluminum widely employed as electrically conductive metals in power transmission, distribution, electric motor windings and electronic devices, is flourishing.

Research spans from producing high-conductivity copper-based materials [1], through metals of higher conductivity such as silver waveguide structures fabricated using Ag nanoparticles [2]. Nanocarbon-based and metal-nanocarbon conductors, too, are promising, though so far their high price justifies use only in aerospace and military applications [3]. In the field of high-conductivity copper-based materials, a significant progress was achieved in 2018 when Zhang and co-workers coated graphene (G) on both sides of a Cu foil obtaining a bulk G/Cu composite conductor having an electrical conductivity 117% higher than pure copper (the International Annealed Copper Standard, IACS) [4].

Subsequent progress was reported in 2022 when a team led by Gao introduced cold drawn Cu/G composite wires of high tensile strength and good electrical conductivity (94.85% IACS) [5]. The composite material was obtained using *in-situ* grown graphene in copper via vacuum hot-press sintering of Cu powder and liquid paraffin. A 2024 account provides a comprehensive review of copper-graphene composite (CGC) conductors, including fabrication processes, electrical performance benchmarks, and copper-graphene interaction mechanisms [6]. Documenting multiple fabrication routes achieving >100% IACS conductivity, said review clearly shows that interface engineering and graphene orientation are critical factors determining electrical conductivity [6].

Methodologies that achieve superior electrical conductivity of CGC include electrodeposition on a copper electrode of graphene nanoparticles suspended in water in the presence of copper sulphate (affording a composite having 15.7% lower resistivity than bare copper) [7]; and friction-based solid-state processing via mechanical graphene dispersion (without chemical synthesis steps), achieving 108% IACS conductivity with 56% tensile strength enhancement [8].

In this study, we report the first investigation of the 3D entrapment of graphene in the crystalline lattice of metals based on the metal organic alloy (MORAL) approach. So far applied to palladium [9,10] and nickel [11,12] obtaining heterogeneous catalysts of largely enhanced performance when compared to the unmodified metal nanoparticles, the method is based on the entrapment of graphene oxide (GO) within crystalline metal lattice via the reduction-precipitation process affording molecularly doped metals [13].

As shown in the following, the GO entrapment in the Cu lattice followed by reduction of entrapped GO to graphene using thiophene, affords a molecularly doped metal (or metal organic alloy, MORAL) named herein "CuproGraf" whose electrical resistivity is 7% lower than that of pure copper made from pure copper powder using the same non-optimized hot rolling method.

2. Results and Discussion

The two-step preparation of CuproGraf (copper-entrapped graphene, G@Cu) employs the entrapment of water-soluble GO within the crystal lattice of Cu through reductive precipitation of copper nitrate driven by an excess of sodium borohydride, followed by reduction of the GO@Cu material with thiophene (Scheme 1).

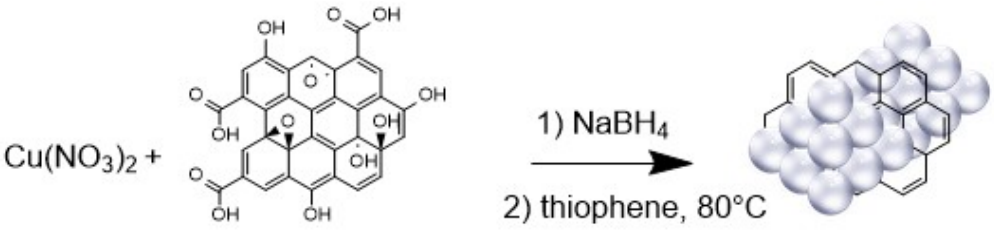

Scheme 1. Synthesis of CuproGraf.

The latter highly effective reduction of the oxidizable functions in GO converts the thiol into an oxidized thiophene polymer, and then to polyhydrocarbon by loss of sulphur atoms, which readily evaporates upon mild heating [14].

The TEM photographs of CuproGraf and the electron diffraction pattern in Figure 1 show that the material is comprised of aggregated rod-shaped Cu nanoparticles with a width equal to 3–5 nm and length in the 15–40 nm range (Figure 1a,d,e).

The presence of graphene layers on the edge of the aggregated nanoparticles (NPs) is evident in all TEM pictures at each magnification degree (Figure 1a–e). In the other regions unveiled by the TEM photographs, the aggregated NPs are tightly intertwined with graphene planes. Electron-diffraction images (Figure 1f) suggest the presence of multiple phases in the material.

The XRD diffractogram of CuproGraf (Figure 2) shows evidence that the material chiefly consists of metallic Cu, with well-defined diffraction peaks around 43.2° and 50.4° originating from the (111) and (200) crystal planes of Cu lattice. Conforming the TEM observations, the presence of entrapped graphene layers is revealed by the diffraction peak at 42.7° relative to the two dimensional (10) reflection of stacking graphene layers [15].

The XRD pattern of as-synthetized CuproGraf shows persistent GO despite thiophene treatment. Incomplete reduction introduces oxygen defects that increase electron scattering.

To obtain a compact metallic bar from CuproGraf powder and carry out the electrical conductivity measurements on this new CGC we employed a hot rolling procedure (See supplementary material). Hot rolling is an established method for consolidating metal powders, including copper matrix composite powders [16]. In the present case, the powder was inserted in a steel tube, that was sealed by pressing the two ends. The different steps of the hot rolling process are summarized in Table 1.

The rolling parameters (temperature, reduction ratio, number of passes) were selected based on preliminary trials to ensure consolidation of both the commercially pure Cu and the CuproGraf powders.

A short video of metallic bar lamination process openly accessible at the URL: https://t.ly/yTYPv. A photograph of the CuproGraf metal bar thereby obtained is displayed in Figure 3. This bar was used to assess the electrical conductivity.

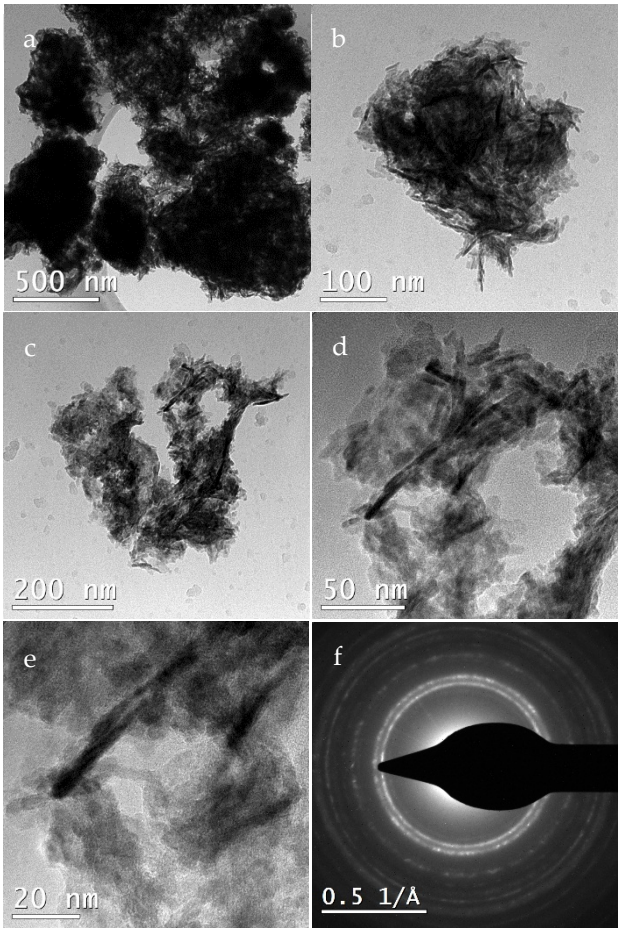

Figure 1. (**a**)–(**e**) TEM photographs of CuproGraf at various degrees of magnification: 500 nm (**a**), 100 nm (**b**), 200 nm (**c**), 50 nm (**d**), 20 nm (**e**) and electron diffraction pattern (**f**).

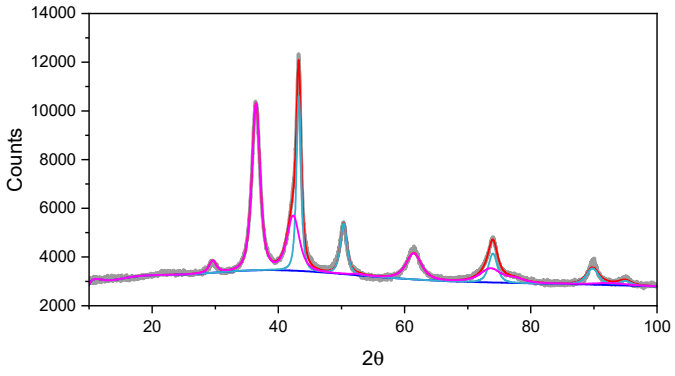

Figure 2. XRD diffractogram of as-synthetized CuproGraf. Raw data, gray line; Cu contribution, light blue line; Cu_2O contribution, pink line; background, blue line; sum of the contribution, red line.

Table 1. Hot rolling parameters.

Powder in a Steel Tube Casing (φ = 12 mm)		
Temperature (°C)	**Time (min)**	**Resulting Diameter (mm)**
800	10	10
800	5	8.5
800	5	7
800	5	6
Bar Is Extracted from the Metal Case (φ = 3 mm)		
800	5	2.7
800	5	2.2

Figure 3. Metallic bars obtained after hot rolling of sintered CuproGraf powder.

The XRD spectrum of CuproGraf in bulk form obtained after hot rolling of sintered CuproGraf powder (Figure 4) no longer shows the presence of residual amounts of copper oxides (CuO and Cu_2O) of as-synthesized CuproGraf powder (Figure 2).

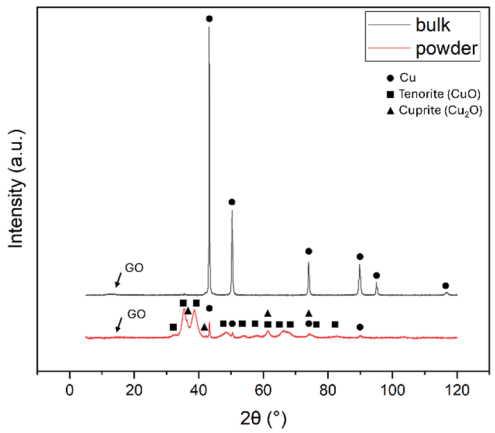

Figure 4. XRD diffractogram of CuproGraf in bulk form obtained after hot rolling of sintered CuproGraf powder.

In brief, during the heat treatment at 800 °C for 10 min of the CuproGraf precursor powder, copper oxides (tenorite, and cuprite) are reduced to metallic Cu due to entrapped graphene acting as reducing agent as it happens when graphene synthesized on copper foil acts as a reducing agent for electroless plating of copper [17].

In brief, the XRD analysis of CuproGraf in bulk form indicates the presence of face-centered cubic copper as the primary phase of CuproGraf, with minor oxidized species and residual graphene oxide (estimated at <2 wt% based on peak intensity ratios). Spectra in Figure 4 highlight that residual GO is present in both the CuproGraf powder and sintered bulk material, regardless of the heterogeneous reduction of GO@Cu with thiophene dissolved in MeOH. On the other hand, the diffraction pattern does not show any peaks associated with iron or iron-containing phases, suggesting that any potential contamination with steel is minimal, and below the detection limit of the technique.

The latter bar in sintered CuproGraf was used to assess the electrical conductivity. Conductivity measurements were performed in triplicate (n = 3 independent batches) with 10 measurements per location. Considering the instruments accuracy and the calculation process, an error in the range of 6%, mainly due to geometrical data, has been estimated for the resistivity measurements reported. Data are reported as mean ± SD.

Remarkably, the resistivity of the CuproGraf bar was 2.06 ± 0.14 mΩ·cm, whereas that of the metallic Cu bar was 2.21 ± 0.133 mΩ·cm, namely 6.78% lower than that of pure copper made from pure copper commercial powder using the same non-optimized method. In other words, the addition of a modest amount (0.5 wt%) of graphene to copper via the moleculary doped metal approach is sufficient to drive a substantial reduction in copper resistivity. The non-optimized hot rolling method employed in this proof of concept study is reflected in the higher resistivity (2.21 ± 0.133 mΩ·cm) for the pure copper bar made from pure copper powder, which corresponds to 45 × 10^6 S/m, or 77.4% IACS (58.1 × 10^6 S/m) [18].

A similar hot rolling procedure was followed to obtain a pure Cu bar from powdered Cu. In detail, a powder sample (18.5 g) of commercial copper (purchased from Sigma Aldrich) consisting of Cu grains 10–45 μm in size was inserted in a metal case similar to that used for the hot rolling of the CuproGraf powder. The bar was mildly polished to remove copper oxide and surface dirt. Figure 5 shows the metal bar eventually obtained.

Figure 5. Metallic bar obtained after hot rolling of sintered Cu.

In other words, regardless of substantially larger size of Cu grains (10–45 μm) for the copper powder used for the hot rolling treatment when compared to submicron CuproGraf particles, and oxide phase presence, the CuproGraf conducting bar (83.7% IACS) shows 6.3% improvement over the processed control copper (77.4% IACS), though both remain below commercially optimized copper standards (>95% IACS).

To further reduce the resistivity and reach in the latter case the IACS resistivity (1.7241 mΩ·cm), sintering of Cu powder into bulk metallic conductor devoid of air's oxygen will require an optimized hot rolling process so as to reduce the porosity of the bulk metallic bar obtained and reduce the grain boundaries. The same optimized hot rolling process would then be applied to the CuproGraf nanstructured powder.

Remarkably, a similar enhancement in the hot-pressing method employed was recently reported as necessary to observe the large enhancement in electrical conductivity of G-Cu multilayered composites produced by G-Cu grains obtained after chemical vapor deposition of graphene [4]. It is also relevant that the aforementioned research was commissioned by the International Copper Association [19].

We briefly remind that in metallic conductors, the resistivity increases with increasing imperfections, such as impurities, grain boundaries, and defects due to additional scattering centers for the electrons carrying the current [20]. Hence, a combined approach to decrease the resistivity Cu is to replace polycrystalline Cu with single-crystal copper [21], followed by concomitant application of heat and pressure after crystal growth to enhance crystallinity [22]. Though affording a single-crystal of Cu having 117.1% IACS, the latter method is not suitable for producing bulk copper wire and foil conductors.

On the other hand, the readily scalable preparation of CuproGraf at low cost may open the route, *inter alia*, to replacement of silver-plated copper in all wires wherein exceptional conductivity is required, such as for example in aircrafts where silver-plated finely-stranded copper wire is employed. Silver indeed is the best conducting metal (≈108% IACS) at room temperature (resistivity of 1.59 mΩ·cm at 293 K). The use of wires consisting of optimally hot rolled CuproGraf would for example eliminate reduction in conductivity due to copper corrosion ("red plague") that affects silver-plated copper wires following reaction between the silver coating, copper, oxygen and water [23].

Though requiring a detailed technoeconomic assessment, the low cost and ease of scalability of CuproGraf fabrication is evident from Scheme 1. All reactants, including GO and thiophene reductant, are low cost reactants available in large amount from numerous chemical suppliers. The MORAL synthetic process is conducted in water, with no by-product formation and nearly complete incorporation of GO, whereas the borohydride anion is an excellent reducing agent of Cu^{2+} promoting the quick and complete conversion of Cu^{2+} into Cu nanoparticles already at [Cu^{2+}] : [BH_4^-] 1:2 ratio (Equation (1)):

$$Cu(NO_3)_2 + 2NaBH_4 + 6H_2O \rightarrow Cu + 7H_2 + 2NaNO_3 + 2B(OH)_3 \quad (1)$$

Nontoxic sodium nitrate, boric acid and hydrogen are the reaction by-products, which makes the process viable at industrial scale for the production, for example, of catalytic Cu NPs using a spinning disk reactor to rapidly micro-mix reactants in order to control nucleation and particle growth for uniform particle size distribution [24].

Finally, the incomplete reduction of graphene oxide (confirmed by the XRD pattern) represents a limiting factor in achieving the theoretical conductivity enhancement and warrants investigation of alternative reduction chemistries (e.g., hydrogen thermal or hydrazine treatment) in future studies.

3. Conclusions

In conclusion, we have discovered that CuproGraf, namely copper doped with 3D-entrapped graphene molecules, is a promising electrical conductor, showing nearly 7% lower resistivity when compared to a copper bar obtained from pure Cu powder using the same non-optimized hot rolling procedure. The bulk conductor formation process, indeed, is still non-optimized achieving a pure copper conductivity 23% lower compared to IACS. The observed 6.78% improvement falls within the measurement error range (±6%), requiring verification through additional characterization. If the difference in resistivity with pure Cu here demonstrated for bulk conductors obtained through the non-optimized metallurgical procedure will be retained, road will be open to wires and foils made of CuproGraf in all applications in which higher conductivity of that achieved using pure Cu is required.

Like any other study, the present study has limitations. The pure copper control achieves only 77.4% IACS (2.21 ± 0.133 μΩ·cm), indicating severe processing defects. CuproGraf (2.06 ± 0.14 μΩ·cm, 83.7% IACS) remains 16.3% below standard copper. Further research needs therefore to explicitly address graphene distribution homogeneity and grain refinement mechanisms in CuproGraf, as well as the development of an optimized compaction procedure within the tube to achieve results comparable to those obtained with pure Cu powder. In addition, copper-graphene composite optimization using rigorous statistical methodology needs to be conducted, along with investigation of alternative reduction methods (i.e., hydrogen thermal, hydrazine) as persistent GO despite thiophene treatment due to incomplete reduction introduces oxygen defects that increase electron scattering. An ample structural investigation including analysis of GO/graphene ratio in CuproGraf via Raman and XPS spectroscopy and the outcomes of a comparative, advanced XRD analysis will be soon reported.

4. Experimental Methods

4.1. CuproGraf Preparation

CuproGraf was prepared by reducing copper nitrate in a GO suspension. In a typical reaction, a 8.2 g aliquot of $Cu(NO_3)_2 \cdot 3H_2O$ (>99.9% pure, purchased from Sigma Aldrich) was dissolved in 80 mL methanol (>99% pure, purchased from VWR) along with 1.4 mL of GO suspension (8 mg/mL) purchased from Nanografi Nano Teknoloji (Istanbul, Turkyie). The mixture was sonicated and filled with N_2, after which an aliquot of sodium borohydride (3.2 g, >96% pure, purchased from Sigma Aldrich) was slowly added under N_2 flow, refrigerating the system in an ice bath. Upon complete addition, the precipitate was filtered on a Büchner vacuum filtration funnel on paper filter, 43–48 μm pore size, washed multiple times with water and methanol, prior to drying under vacuum at room temperature.

The 0.5 wt% graphene content in CuproGraf was estimated from precursor amounts, based on full retention efficiency percentage (namely assuming ~100% retention through synthesis and processing), as it happens in most MORALs preparative routes [25].

The procedure was repeated to obtain an amount suitable for the sintering process. For the reduction of GO entrapped in the crystal lattice of Cu, a 20 g sample of GO@Cu in a round bottom flask was added with 150 mL methanol and 5 mL thiophene (>99% pure, purchased from Sigma Aldrich). The flask atmosphere was filled with nitrogen and the mixture heated at 80 °C for 24 h. The final material was filtered using a Büchner vacuum filtration funnel, and extensively washed with methanol, prior to drying under vacuum at room temperature.

4.2. Preparation of CuproGraf and Cu Metallic Bars

Two metallic conductors were prepared using identical hot-rolling treatment: one made of pure copper and one of CuproGraf. A smaller quantity of CuproGraf powder was employed in comparison to copper powder due to the greater difficulty in compacting nanometric powders compared to the micrometric copper powder. In detail, in the case of the copper conductor, a copper powder, 18.55 g of Cu powder (Sigma Aldrich, particle size between 10–45 μm) was loaded into a metal casing with an outer diameter of 12 mm and an inner diameter of 9 mm, with

the powder filling approximately 65 mm of the tube length. In the case of the CuproGraf conductor, 6.05 g of CuproGraf powder, consisting of finer nanometric particles, was used for the same hot-rolling treatment. The aliquot (6.05 g) of CuproGraf powder was filled into a steel tube with an outer diameter of 12 mm, an inner diameter of 9 mm, and a total length of 81 mm. The tube underwent a sequence of heating and rolling steps aimed at sintering the powder and progressively reducing the thickness of the sample. The external steel casing was then removed, and a compact copper bar was extracted. Hot rolling was then continued. The tubes filled with powder were heated in a furnace at 800 °C for 10 min, after which they underwent a series of heating and rolling steps to progressively reduce the material thickness.

The resulting compacted bars, measuring approximately 57 × 10 × 3.3 mm, were extracted from the metal casings. These bars were then subjected to further heating and rolling, reducing their thickness down to 2.2 mm. During processing, visible cracks appeared on the sample surfaces, which were already present after extraction from the metal casings. To prevent crack propagation during the subsequent rolling steps, the samples were lightly polished.

4.3. Structural Characterization

The transmission electron microscopy (TEM) experiments were carried out using a Thermo Fisher Scientific Talos L120C instrument operating at 120 kV. Samples were deposited on Cu-grids as such. The XRD diffractograms were obtained using a Rigaku Miniflex 600 diffractometer with Cu Kα radiation (λ = 0.1541 nm), acquiring data in the 10–100° 2θ range with a step size of 0.05° and a counting time of 8 s per step.

4.4. Resistivity Measurements

The resistance measurements were conducted using a Resistomat Typ 2305 at room temperature (approx. constant at 295 K). Considering the low values for resistance expected for the samples, the system has been equipped with Kelvin clips to decouple I–V contacts, preventing systematic errors associated to contact resistance. At the same time, the measurements have been performed applying a current cycle to the sample alternating I direction with a frequency of 1, 5 and 10 Hz: this allows to discard errors due to offsets and thermal effects. Data were collected on pure copper sample obtained by powdered Cu hot lamination, used as reference, and on CuproGraf sample.

Resistivity was calculated using the samples measured size for the cross section and the distance between the contacts: the irregular shape of the CuproGraf sample was polished to obtain a more regular geometry. The resulting size ranged between 2.622 and 2.690 mm in width and 0.786 and 0.789 mm in thickness. Results reported are the average of 10 measurements repeated for 3 different distances between the contacts integrating the data collected during 10 s cycling. Considering the instruments accuracy and the calculation process, an error in the range of 6%, mainly due to geometrical data, has been estimated for the resistivity measurements reported.

Author Contributions

M.P., C.D.P., R.C. (Rosaria Ciriminna), M.F.: conceptualization, methodology, formal analysis; R.C. (Riccardo Casati), C.F., G.L., M.F.: methodology, data curation, formal analysis, software; M.P: writing—original draft preparation; R.C. (Riccardo Casati), G.L., M.F., C.F.: visualization, investigation, software; C.D.P., M.P., C.D.P., R.C. (Rosaria Ciriminna), C.F, R.C. (Riccardo Casati): resources; C.D.P., M.P., R.C. (Riccardo Casati): supervision; C.D.P., M.F., R.C. (Rosaria Ciriminna), G.L., R.C. (Riccardo Casati), C.F: writing—reviewing and editing. All authors have read and agreed to the published version of the manuscript.

Funding

We thank the Università degli Studi di Milano PSR2023_DIP_005_PI_MSTUC project for funding the PhD grant of one of us (M.F.). M.P. and R.C. thank the Ministero delle Imprese e del Made in Italy under the Piano Operativo della Ricerca “Ricerca e sviluppo sull’idrogeno” financially supported by the European Union—NextGenerationEU—M2C2 Investment 3.5, in the framework of the project PNRR Ricerca e Sviluppo sull’Idrogeno 2022–2025—Accordo di Programma “Idrogeno” (PRR.AP015.017.002), “Obiettivo 1—Produzione di idrogeno verde e pulito,” “LA 1.1.6—Sviluppo di materiali e componenti non contenenti materiali critici per elettrolizzatori anionici (AEM) operanti anche ad elevata pressione differenziale”.

Data Availability Statement

All data are available upon reasonable request by contacting the corresponding Authors.

Conflicts of Interest

The authors declare no conflict of interest.

Use of AI and AI-assisted Technologies

No AI tools were utilized for this paper.

References

1. Zhang, W.-J.; Huang, L.; Mi, X.-J.; et al. Researches for higher electrical conductivity copper-based materials. *cMat* **2024**, *1*, e13. https://doi.org/10.1002/cmt2.13.
2. Alshehri, H.; Jakubowska, M.; Młożniak, A.; et al. Enhanced electrical conductivity of silver nanoparticles for high frequency electronic applications. *ACS Appl. Mater. Interfaces* **2012**, *4*, 7007–7010. https://doi.org/10.1021/am3022569.
3. Tehrani, M. Advanced electrical conductors: An overview and prospects of metal nanocomposite and nanocarbon based conductors. *Phys. Status Solidi A* **2021**, *218*, 2000704. https://doi.org/10.1002/pssa.202000704.
4. Cao, M.; Xiong, D.; Yang, L.; et al. Ultrahigh electrical conductivity of graphene embedded in metals. *Adv. Funct. Mater.* **2019**, *29*, 1806792. https://doi.org/10.1002/adfm.201806792.
5. Gao, Z.; Zuo, T.; Wang, M.; et al. *In-situ* graphene enhanced copper wire: A novel electrical material with simultaneously high electrical conductivity and high strength. *Carbon* **2022**, *186*, 303–312. https://doi.org/10.1016/j.carbon.2021.10.015.
6. Yao, J.; Kim, C.; Nian, Q.; et al. Copper-graphene composite (CGC) conductors: Synthesis, microstructure, and electrical performance. *Small* **2024**, *20*, 2403241. https://doi.org/10.1002/smll.202403241.
7. Almonti, D.; Salvi, D.; Ucciardello, N.; et al. Enhanced wear resistance and thermal dissipation of copper–graphene composite coatings via pulsed electrodeposition for circuit breaker applications. *Materials* **2024**, *17*, 6017. https://doi.org/10.3390/ma17236017.
8. Khorram, D.; Elyasi, M.; Mirnia, M.J.; et al. Characterization of copper–graphene nanocomposite block prepared by friction stir additive manufacturing. *Prog. Addit. Manuf.* **2025**, *10*, 6805–6824. https://doi.org/10.1007/s40964-025-01008-5.
9. Formenti, M.; Pagliaro, M.; Della Pina, C.; et al. Graphene oxide in palladium nanoparticle (GrafeoPlad): A new class of functional materials. *Green Synth. Catal.* **2025**, *6*, 297–301. https://doi.org/10.1016/j.gresc.2024.04.004.
10. Formenti, M.; Casaletto, M.P.; Barone, G.; et al. GrafeoPlad palladium: Insight on structure and activity of a new catalyst series of broad scope. *Adv. Sustain. Syst.* **2024**, *8*, 2300643. https://doi.org/10.1002/adsu.202300643.
11. Pagliaro, M.; Pagliaro, M.V.; Caliandro, R.; et al. NiGraf: A new nickel-based molecularly doped metal for enhanced water electrolysis. *Mater. Adv.* **2024**, *5*, 2759–2766. https://doi.org/10.1039/d3ma00700f.
12. Formenti, M.; Ciriminna, R.; Della Pina, C.; et al. Reduced NiGraf: An effective hydrogenation catalyst of large applicative potential. *Next Mater.* **2025**, *8*, 100751. https://doi.org/10.1016/j.nxmate.2025.100751.
13. Behar-Levy, H.; Avnir, D. Entrapment of organic molecules within metals: Dyes in silver. *Chem. Mater.* **2002**, *14*, 1736–1741. https://doi.org/10.1021/cm011558o.
14. Some, S.; Kim, Y.; Yoon, Y.; et al. High-quality reduced graphene oxide by a dual-function chemical reduction and healing process. *Sci. Rep.* **2013**, *3*, 1929. https://doi.org/10.1038/srep01929.
15. Stobinski, L.; Lesiak, B.; Malolepszy, A.; et al. Graphene oxide and reduced graphene oxide studied by the XRD, TEM and electron spectroscopy methods. *J. Electron Spectrosc. Relat. Phenom.* **2014**, *195*, 145–154. https://doi.org/10.1016/j.elspec.2014.07.003.
16. Wang, Y.-L.; Wang, K.-K.; Wang, Y.-W.; et al. Experiment and simulation for rolling of diamond–Cu composites. *Acta Metall. Sin.* **2017**, *30*, 791–800. https://doi.org/10.1007/s40195-017-0561-z.
17. Narula, U.; Tan, C.M.; Tok, E.S. Metal on graphenated metal for VLSI interconnects. *Adv. Mater. Interfaces* **2018**, *5*, 1800270. https://doi.org/10.1002/admi.201800270.
18. *ASTM B193-20*; Standard Test Method for Resistivity of Electrical Conductor Materials. ASTM International: West Conshohocken, PA, USA, 2014. https://doi.org/10.1520/b0193.
19. International Copper Association. Ultra-Conductive Copper Development in China, Final Report. Projects TEK-1064-SJTU and MDP-1268-HA, August 2014–August 2016. Available online: https://internationalcopper.org/wp-content/uploads/2021/08/report-ultra-conductive-copper-development.pdf (accessed on 10 November 2025).
20. Bakoniy, I. Accounting for the resistivity contribution of grain boundaries in metals: Critical analysis of reported experimental and theoretical data for Ni and Cu. *Eur. Phys. J. Plus* **2021**, *136*, 410. https://doi.org/10.1140/epjp/s13360-021-01303-4.
21. Cho, Y.C.; Lee, S.; Ajmal, M.; et al. Copper better than silver: Electrical resistivity of the grain-free single-crystal copper wire. *Cryst. Growth Des.* **2010**, *10*, 2780–2784. https://doi.org/10.1021/cg1003808.

22. Ajmal, M. Fabrication of the best conductor from single-crystal copper and the contribution of grain boundaries to the Debye temperature. *CrystEngComm* **2012**, *14*, 1463–1467. https://doi.org/10.1039/c1ce06026k.
23. Company, L.D. For Aircraft Wire Systems, There Is No Perfect Conductor, Not Even a Silver Plated One, 1 July 2006. Available online: https://lectromec.com/for-aircraft-wire-systems-there-is-no-perfect-conductor-not-even-a-silver-plated-one/ (accessed on 5 December 2025).
24. Ahoba-Sam, C.; Boodhoo, K.V.K.; Olsbye, U.; et al. Tailoring Cu nanoparticle catalyst for methanol synthesis using the spinning disk reactor. *Materials* **2018**, *11*, 154. https://doi.org/10.3390/ma11010154.
25. Avnir, D. Molecularly doped metals. *Acc. Chem. Res.* **2014**, *47*, 579–592. https://doi.org/10.1021/ar4001982.